Food Hydrocolloids 73 (2017) 235–242

Contents lists available at ScienceDirect

Food Hydrocolloids

journal homepage: www.elsevier.com/locate/foodhyd

Sequencing analysis of β-glucan from highland barley with high performance anion exchange chromatography coupled to quadrupole time − Of − Flight mass spectrometry

Yinxiu Rong [a], Naiyu Xu [a, **], Bingying Xie [a], Jie Hao [a], Lin Yi [a], Ruomei Cheng [a], Duxin Li [a], Robert J. Linhardt [b], Zhenqing Zhang [a, *]

[a] Jiangsu Key Laboratory of Translational Research and Therapy for Neuro-Psycho-Diseases, College of Pharmaceutical Sciences, Soochow University, Suzhou, Jiangsu, 215021, China
[b] Center for Biotechnology and Interdisciplinary Studies, Rensselaer Polytechnic Institute, 110 8thStreet, Troy, NY, 12180, USA

ARTICLE INFO

Article history:
Received 7 May 2017
Received in revised form
4 July 2017
Accepted 5 July 2017
Available online 6 July 2017

Keywords:
Highland barley
β-glucan
Sequence analysis
HPACE-PAD
MS/MS

ABSTRACT

Highland barley is one of the hull-less barleys that contains high amounts of β-glucan. A detailed sequence analysis is needed to support the application of the β-glucan from highland barley. The β-conformation and 1 → 3/1 → 4 linkages were confirmed using nuclear magnetic resonance (NMR) spectroscopy. Monosaccharide analysis was accomplished with high-performance anion exchange chromatography (HPAEC) coupled to pulsed amperometric detection (PAD) and showed that glucose (G) was the dominant sugar component of this β-glucan. HPAEC-PAD was applied with on-line electrospray ion - to quadrupole time − of − flight mass spectrometry (Q/TOF-MS) to sequence oligosaccharides enzymatically derived from this β-glucan. More than 20 oligosaccharides were observed in the partially digested β-glucan mixture and their degree of polymerization (dp), confirmed by MS analysis, ranged from dp 2 to dp 20. The sequences of oligosaccharide dp2 − dp7 in the digested product mixture were unambiguously determined with MS/MS. Based on the sequence analysis of these oligosaccharides, G1→3G1→4G and G1→3G1→4G1→4G were determined to be the major repeating blocks of this β-glucan, and they were interspersed with homogeneous 1 → 4 linked domains with different lengths. The ratio of 1 → 3 and 1 → 4 linkages in the β-glucan was approximately 1:3.

1. Introduction

Cereals, including wheat, barley, oat, and rice, serve as a major source of food-derived energy for millions of people worldwide. Barley is considered as 'health food' for humans even though it is consumed in considerably lower quantities than are wheat and rice (Gangopadhyay, Hossain, Rai, & Brunton, 2015). Highland barley, an important hull-less barley, is the staple food crop on the Qinghai-Tibet Plateau in China (Yang, Christensen, McKinnon, Beattie, & Yu, 2013; Zhu, Du and Xu, 2015). With the discovery that barley possesses bioactivities largely attributable to its soluble fiber fraction, in particular its higher content of β-glucan, investigations into its use as a functional food has been intensified (Anderson et al., 1991; Gangopadhyay et al., 2015; Åman, 2006).

The β-glucan of highland barley is a glucopyranose-containing polysaccharide found in the cell walls of the grain's endosperm (Lam & Chi-Keung Cheung, 2013; Lopez-Sanchez, Wang, Zhang, Flanagan, & Gidley, 2016; Peng, Peng, Xu, & Sun, 2012; Razzaq et al., 2016; Zhao & Cheung, 2013). Data suggests that this β-glucan is a potent immunomodulator with effects on innate and adaptive immunity (Schulze et al., 2016; Shao, Wang, Tian, Guo, & Zhang, 2016), which might be applied as a potential drug in the cancer therapy. Other reports show the hypolipidemic and hypoglycaemic effects of barley β-glucan (Bae, Kim, Lee, & Lee, 2010; Dong, Cai, Shen, & Liu, 2011; Drozdowski et al., 2010; Liu et al., 2016; Thondre & Henry, 2009; Tiwari & Cummins, 2011; Tong et al., 2015; Zhu et al., 2015). This β-glucan can regulate blood lipid through forming a highly viscous mass in the intestine, limiting intestinal absorption of cholesterol in food as well as the re-absorption of bile acids. This subsequently leads to the up-regulation of low density lipoprotein receptor (LDLR) and increases conversion of cholesterol to bile acids

* Corresponding author.
** Corresponding author.
E-mail address: z_zhang@suda.edu.cn (Z. Zhang).

http://dx.doi.org/10.1016/j.foodhyd.2017.07.006
0268-005X/

(Bae, Lee, Kim, & Lee, 2009; Mikkelsen, Jespersen, Larsen, Blennow, & Engelsen, 2013). As a result, the β-glucan is known to be effective in lowering low-density lipoprotein (LDL) and cholesterol (Gangopadhyay et al., 2015; Lam & Chi-Keung Cheung, 2013; Lehtovaara & Gu, 2011; Yoshida, Honda, Tsujimoto, Uyama, & Azuma, 2014), without affecting cholesterol metabolism in young-healthy adults (Ibrugger et al., 2013). Furthermore, a number of investigations have shown the anti-diabetic properties of the β-glucan (Dong et al., 2011; Liu et al., 2016; Thondre & Henry, 2009; Uskoković et al., 2013). β-glucan is also a potential α-glycosidase inhibitor, decreases the absorption of glucose in small intestine (Dong et al., 2011), and is capable of controlling the level of plasma glucose and improving hepatogenic glycometabolism in streptozotocin-nicotinamide induced mice (Liu et al., 2016).

More detailed information on the structure and sequence of highland barley β-glucan is required to effectively exploit its various pharmacological activities. The major structure of barley β-glucan reportedly contains some β-(1 → 3) linked glucose residues with a predominance of β-(1 → 4) linked linear glucan chains. Nuclear magnetic resonance (NMR) spectroscopy is typically widely-used to elucidate the structure of complex polysaccharides. However, NMR requires a large quantity of highly pure sample for analysis, and while providing structural information, it affords little information on polysaccharide sequence. A trisaccharide and a tetrasaccharide are reportedly present in enzymatically digested products of barley β-glucan (Ghotra, Vasanthan, & Temelli, 2008). Their detailed structures were elucidated with NMR, which confirmed the presence of a small amount of β-(1 → 3) linked glucose among the dominant β-(1 → 4) linked glucan chains. However, no additional structural or sequence information on other oligosaccharide domains present in this β-glucan were obtained since the preparation of sufficient amounts of oligosaccharides is both time and labor intensive. Moreover, the structural elucidation of oligosaccharide with NMR is typically quite complicated with severe signal overlap. Consequently, highland barley β-glucan can still not be sequenced solely using NMR spectroscopy.

A hyphenated method in which high-performance anion exchange chromatography (HPAEC) with pulsed amperometric detection (PAD) is coupled to electrospray ion quadrupole time − of − flight mass spectrometry (ESI-Q/TOF-MS) was developed to begin the online sequencing of these oligosaccharides in our laboratory (Schmidt et al., 2016; Yi, Ouyang et al., 2015). Using this method, the oligosaccharide domains of glucans could be separated using high resolution HPAEC, semi-quantified using PAD and sequenced using MS/MS. All these analyses could be accomplished online to elucidate the structure of enzymatically digested β-glucan extracted from highland barley. The different oligosaccharide domains in partially digested products were analyzed using this approach and the sequence of β-glucan from highland barley is described.

2. Materials and experiments

2.1. Materials

Highland barley was harvested at Tibet in Sep. 2016. Beta-glucanase was purchased from Yuanye Bio-technology Co., Ltd (Shanghai, China). Heat stable α-amylase was obtained from Aladdin (Shanghai China). High-purity water (resistivity ≥18.2 MΩ × cm, 25 °C) was used throughout the study. All other chemicals and reagents were of LC-MS grade.

2.2. Preparation of β-glucan from highland barley

The β-glucan was extracted from highland barley partially following the previously reported method (Tosh, 2004). Highland barley powder (100 g) was first pretreated by refluxing with 800 mL 80% ethanol for 2 h to remove alcohol-soluble solids and denature some of the enzymes present in the barley. The ethanol-extracted residue was oven dried. Pure water (450 mL) and 1 mL 20% Na_2CO_3 (w/w) solution were added to the ethanol pre-treated highland barley powder (30 g). The mixture was incubated at 85 °C for 2 h with continuous stirring. Heat stable α-amylase (135 units) was then added and the mixture was incubated with stirring at 90 °C for 2 h. The reaction was cooled down to room temperature and its pH was adjusted to 4.5 with 1 M HCl solution, denaturing most of proteins and enzymes. The precipitate was removed by centrifuging at 4500 rpm for 20 min. The supernatant was recovered and concentrated to 150 mL and 75 g ammonium sulfate was added with continuous stirring. The solution was kept overnight at 4 °C, to precipitate the crude β-glucan. Crude β-glucan was collected by centrifugation at 4500 rpm for 15 min. The pure β-glucan was obtained by repeating the above procedures. The dried pure β-glucan could be dissolved in hot water and would not be separated out from solution when it is cool down to room temperature.

2.3. Monosaccharide composition analysis with HPAEC-PAD (Zhang, Khan, Nunez, Chess, & Szabo, 2012)

Monosaccharide analysis with HPAEC-PAD was applied to confirm the compositional purity of the extracted sample. The extracted polysaccharide sample was depolymerized with 2 M trifluoroacetic acid (TFA) at 100 °C for 12 h. After removal of the excess TFA by evaporation under vacuum, the monosaccharides in the hydrolysate were analyzed with HPAEC-PAD. The experiment was performed on a Metrohm 850 Professional system equipped with a 919 IC auto-sampler plus, dual pumps and a PAD (Herisau, Switzerland). Hydrolysate was analyzed on a CarboPac PA-1 column (4 × 250 mm, Dionex, Sunnyvale, CA) at a flow rate of 1 mL/min and 30 °C with isocratic gradient (15 mM NaOH).

2.4. ^{13}C NMR analysis

Sample (50 mg) was dissolved in 1.5 mL D_2O (99.9 atom %) for NMR analysis. The ^{13}C experiment was acquired on a 600 MHz NMR spectrometer (Agilent, CA, USA) with 10240 scans and temperature at 298 K. The data was processed with MestReNova software of version 6.1.1.2.2.4.

2.5. Depolymerized by beta-glucanase

About 3 mg β-glucan was dissolved in a proper volume of PBS buffer (pH 6.8) to afford to a final concentration of 3 mg/mL. The solution was incubated with ~1 U of β-glucanase at 40 °C. The aliquots were taken at 6, 12 and 24 h. Boiling each aliquot for 20 min terminated the action of the enzyme. The denatured enzyme was removed by centrifugation for 10 min at 15,000 rpm.

2.6. HPAEC setup

HPAEC-PAD analysis was performed on a Metrohm 850 profession system equipped with dual pump. Each aliquot (20 μL) was separated with a CarboPac PA-200 column (3 × 250 mm, Dionex, Sunnyvale, CA) at a flow rate of 0.8 mL/min. Mobile phase A is 100 mM NaOH, mobile phase B is 1 M NaOAc in 100 mM NaOH solution. A linear gradient from 0% to 35% of mobile phase B was applied during 35 min.

2.7. Desalting

The eluent after the column is split using a T-piece, in which 62.5% of the eluent went to PAD (0.5 mL/min), and 37.5% of the eluent (0.3 mL/min) went to the desalter, based on a suitable MS flow rate. The ratio of splitting was selected based on the back-pressures from these two pathways, which were adjusted by selecting the diameters and lengths of tubes. An ion suppressor MSM-HCRotor A (Metrohm, Switzerland) was used to remove sodium before MS analysis. There were three cation-exchange cartridge units installed in this column array. The detailed flow chart and mechanism of this desalter was described in our previous work (Yi, Ouyang et al., 2015).

2.8. MS parameters

Nitrogen gas was used in the nebulizer at a pressure of 40 psi as drying gas. The flow rate of nitrogen gas was 10 L/min at 350 °C in the drying process and the voltage was set at 3.5 kV. The fragment voltage was set to 100 V. A full MS scan between 100 and 2000 m/z was performed. The collision-induced dissociation (CID) energies used in MS/MS to dissociate disaccharide, trisaccharide, tetrasaccharide, pentasaccharide, hexasaccharide and heptasaccharide were set as 15–40 V according to different molecular mass. All data were acquired at negative ion mode with Mass Hunter 6.0 (Agilent Technologies).

3. Results

Monosaccharide standards were well separated on the column and included arabinose, galactose, glucose and xylose (Fig. S1). Compared with the chromatograms of monosaccharide standards, the retention time of analyte in the hydrolysate of extracted polysaccharide were consistent with glucose and no other peaks were observed in the chromatogram (Fig. S1), demonstrating that the extracted polysaccharide was a pure glucan and other heteropolysaccharides had all been removed. The monosaccharide composition of side-product was also confirmed with HPAEC-PAD. The two major peaks corresponding to arabinose and xylose were observed, suggesting it contains a big amount of araboxylan. The detailed results of the monosaccharide analysis are shown in the supplementary data.

The negative results of chromogenic reaction with iodine solution also confirmed that starch had been completely removed by treatment with α-amylase. Overall, about 1.6 g pure β-glucan were prepared from 100 g dried highland barley powder.

Table 1
^{13}C NMR Assignments for barley β-glucan from highland barley.

Glucosyl residue (Glcp)	^{13}C Chemical shifts, ppm					
	C-1	C-2	C-3	C-4	C-5	C-6
β-(1 → 3)	104.03	73.38	87.71	71.04	76.70	61.24
β-(1 → 4)	103.20	68.72	72.63	80.74	75.37	60.69

3.1. ^{13}C NMR analysis of pure β-glucan

The ^{13}C NMR spectrum of prepared sample is shown in Fig. 1. According to previous reports (Johansson et al., 2000), including the assignments in the regular ^{13}C NMR spectrum of curdlan, a pure β-(1 → 3) linked glucan (Lehtovaara & Gu, 2011), and the assignments in the solid-state ^{13}C NMR spectrum of cellulose, a pure β-(1 → 4) linked glucan (Idstrom et al., 2016), the ^{13}C NMR spectrum of the glucan extracted from highland barley was assigned. The assignments are presented in Table 1. The resonance at 104.03 ppm was assigned as C-1 carbon of the β-(1 → 3) linkage. The resonance at 103.20 ppm was assigned to C-1 carbon of the β-(1 → 4) linkage. The C-3 carbon of the β-(1 → 3) linkage was observed at 87.71 ppm. The resonance at 73.38, 71.04, 76.70 and 61.24 ppm were identified, respectively, corresponding to C-2, C-4, C-5 and C-6 of the O-3-β-glucose residues. The resonance at 68.72, 72.63, 80.74, 75.37 and 60.69 ppm were assigned to C-2, C-3, C-4, C-5 and C-6 carbons of the O-4-β-glucose residue, respectively.

Thus, we confirmed that the prepared glucan from highland barley is β-glucan and it contains some β-(1 → 3) linked glucose residues among the predominant β-(1 → 4) linked linear glucan chains. According to the integral proportion of the peaks corresponding to anomeric carbons of 1 → 3 and 1 → 4 linked sugar residues in ^{13}C NMR spectrum, the ratio of 1 → 3 and 1 → 4 linkages was measured as 1:2.9.

3.2. HPAEC-PAD-MS analysis of digested products

Three aliquots taken at 6, 12 and 24 h of enzymatic digestion were analyzed with HPAEC-PAD-MS. Their PAD chromatograms are shown in Fig. 2. The degree of polymerization (dp) of oligosaccharides corresponding to each peak in the PAD chromatograms were assigned based on MS analysis and are labeled in Fig. 2. The molecular weights of the observed oligosaccharides were used to extract the total ion chromatograms (TICs). The extracted ion chromatograms (EICs) are shown as inserts of Fig. 2. The MS spectrum of each peak was shown in the supplementary data. (Fig. S2) In the MS spectra of oligosaccharides dp2–dp9 show singly charged molecular ions $[M-H]^-$ as the major signals. The

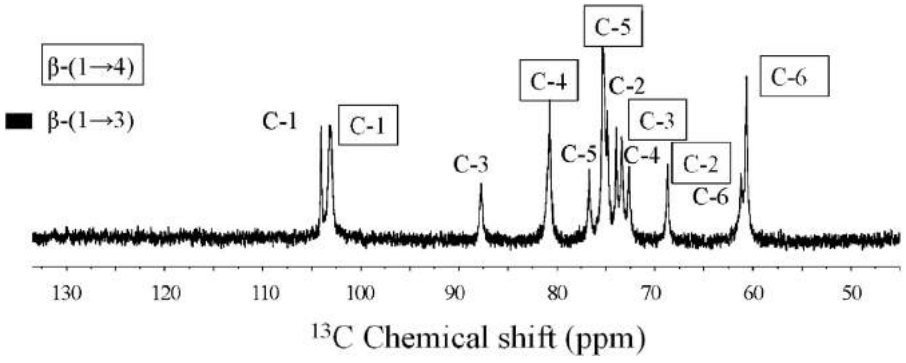

Fig. 1. ^{13}C NMR spectrum of purified β-glucan from highland barley.

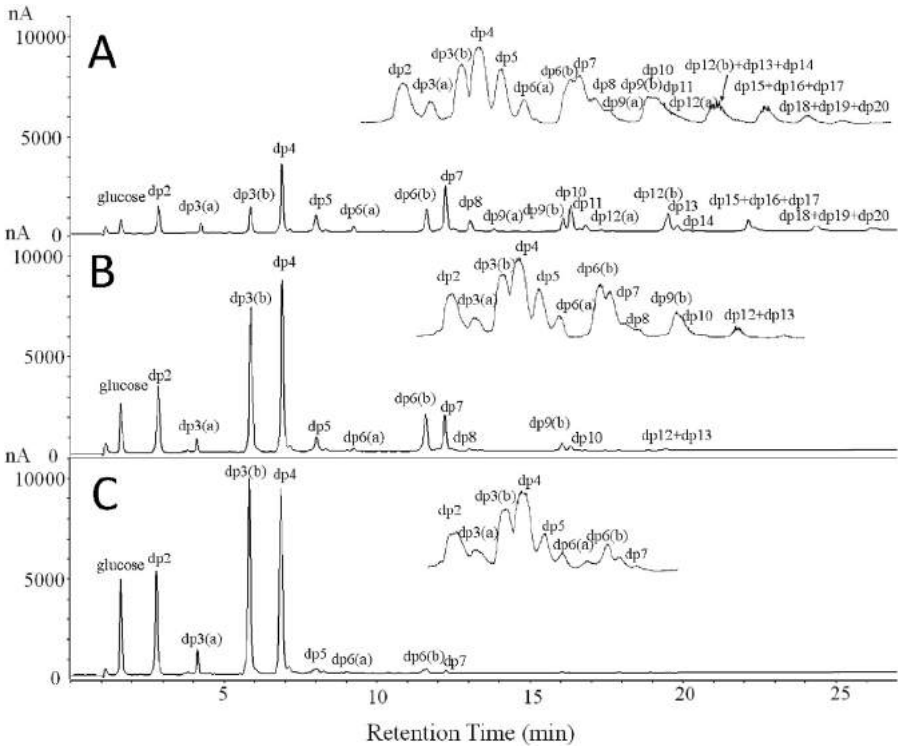

Fig. 2. The PAD chromatograms with its corresponding EIC of aliquots taken at 6 h, 12 h and 24 h.

doubly charged molecular ions $[M-2H]^{2-}$, dominate the MS spectra of dp11–dp20. In addition, adducts molecular ions containing two water molecules, $[M+2H_2O-H]^-/[M+2H_2O-2H]^{2-}$, or one HSO_4^-, $[M+HSO_4^-]^-/[M-H+HSO_4^-]^{2-}$, were always present along with $[M-H]^-$ or $[M-2H]^{2-}$. Dilute H_2SO_4 solution, used to wash the cation exchange cartridge column in the online desalter apparently results in the present of hydrogen sulfate groups as adducts ion in the MS analysis (Yi, Ouyang et al., 2015). The EIC profile of each sample was similar to the PAD results. However, as the presence of large dead volume in desalter before the eluent enters the mass spectrometer results in broader peaks in the EICs than observed in the PAD chromatograms.

More than 20 peaks were observed in the PAD chromatogram of aliquot taken at 6 h (Fig. 2A). The peaks corresponding to glucose, disaccharide (dp2), dp4, dp5, dp7, dp8, dp10, and dp11 were observed at 1.7, 2.8, 6.9, 8.0, 12.2, 13.0, 16.4 and 17.0 min, respectively. The oligosaccharides dp3, dp6, dp9 and dp12 were all observed as double peaks, and labeled as (a) and (b). The oligosaccharides dp15-17 and dp18-20 eluted together, demonstrating a limitation in the resolution of this method. The intensities of the peaks corresponding to bigger oligosaccharides decreased, while those of glucose, dp2, dp3(b) and dp4 increased in the chromatogram of 12 h aliquot (Fig. 2B). When the digestion time was increased to 24 h, the peaks of glucose, dp2, dp3(b) and dp4 dominated the chromatogram (Fig. 2C).

3.3. MS/MS analysis of oligosaccharides in digested products

MS/MS was performed on the peaks corresponding to dp2-dp7 observed in PAD chromatograms and the fragment ions produced were used to sequence each oligosaccharide. The assignments of molecular ions and fragment ions in their MS/MS spectra were made utilizing the nomenclature of Domon and Costello (Domon, 1988). The MS/MS spectrum of disaccharide is shown in Fig. 3A. Typical glycosidic bond cleavage ions, such as B_1 (m/z 161)/C_1 (m/z 179), and two cross ring cleavage ions, $^{2,4}A_2$ (m/z 221)/$^{2,5}A_2$ (m/z 263), were assigned in the MS/MS spectrum and labeled on the structure. The assignments are also listed in Table 2. The 1 → 4 linkage pattern of dp2 was confirmed with the presence of the bond 2 cleavage in the sugar ring involved cross ring cleavage ions, $^{2,4}A_2$ (m/z 221)/$^{2,5}A_2$ (m/z 263) (Yi, Ouyang et al., 2015; Yi, Sun et al., 2015).

MS/MS was next employed to confirm the sequences of two trisaccharides (Fig. 3B and C). In addition to glycosidic bond cleavage ions, B and C fragment ions, two diagnostic cross-ring cleavage ions, $^{2,5}A_2$ (m/z 263) and $^{2,5}A_3$ (m/z 425), were observed in the spectrum of dp3(a). These indicate that the two linkages of this trisaccharide are all 1 → 4, and the sequence of dp3(a) is G1→4G1→4G. As we previously reported (Yi, Ouyang et al., 2015; Yi, Sun et al., 2015), the absence of cross-ring cleavage ions suggests the 1 → 3 linkage. No observation of cross-ring ions at the second residue from the non-reducing end of dp3(b) certifies its 1 → 3 linkage (Fig. 3C). The presence of the 1 → 4 linkage diagnostic cross-ring ions, $^{2,4}A_3$ (m/z 383)/$^{2,5}A_3$ (m/z 425)/$^{0,2}A_3$ (m/z 443), at the reducing end residue in the dp3(b) spectrum, in which the bond 2 in sugar ring is involved, confirms a 1 → 4 glycosidic bond. The assignments are also provided in Table 2. The sequence of dp3(b) was determined to be G1→3G1→4G.

In the MS/MS spectrum of dp4 (Fig. 3D), the presence of diagnostic ions, $^{2,5}A_3$ (m/z 425) and $^{2,5}A_4$ (m/z 587), suggests both of the third and fourth residues from non-reducing end are 1 → 4 linked glucose residues. The same as observed in the spectrum of dp3(b), the absence of cross-ring fragment ions at the second glucose residue demonstrates the 1 → 3 linkage. The assignments are listed in Table 2. The sequence of dp4 was identified as G1→3G1→4G1→4G. The sequences of dp3(b) and dp4 elucidated in this work are consistent with the results previously reported using NMR spectroscopy (Ghotra et al., 2008).

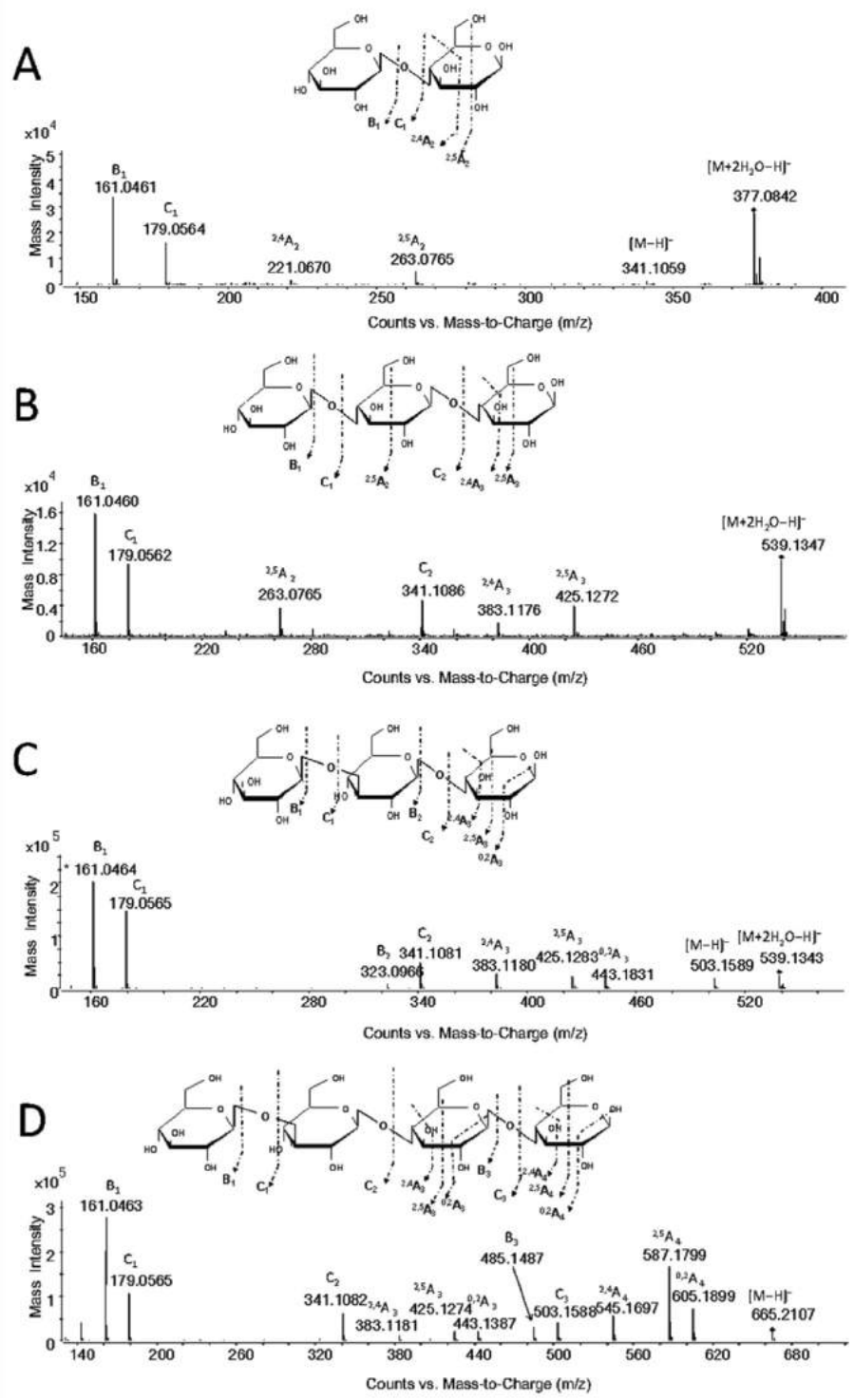

Fig. 3. MS/MS spectra of dp2, dp3(a), dp3(b) and dp4.

According to the different patterns of cross-ring cleavage ions in their MS/MS spectra corresponding to 1 → 3 and 1 → 4 linkages, respectively, the sequences of dp5, dp6(a), dp6(b) and dp7 were confirmed (Fig. 4). Their assignments are presented in Table 2. Their sequences are G1→[4G1]$_3$→4G, Glc1→[4G1]$_4$→4G, G1→3G1→[4G1]$_2$ → 3G1→4G and G1→3G1→[4G1]$_2$ → 3G1→4G1→4G. The quality of MS/MS spectra of larger oligosaccharides was not sufficient to confirm their sequences due to the limitation of chromatographic resolution and detection sensitivity of Q/TOF-MS.

4. Discussion and conclusion

In our previous reports, the glycosidic linkage to position 3 of the 1 → 3 linked sugar ring stabilized the bonds 2 and 3 on the sugar ring, which are the most active bonds to be dissociated in MS/MS. Thus, the cross-ring fragmentation ions are rarely observed in

Table 2
Assignments of fragment ions in MS/MS spectra for different oligosaccharides.

	Precursor ions (m/z)[a]	B_1	C_1	$^{2,4}A_2$	$^{2,5}A_2$	B_2	C_2	$^{2,4}A_3$	$^{2,5}A_3$	$^{0,2}A_3$	B_3	C_3	$^{2,4}A_4$	$^{2,5}A_4$	$^{0,2}A_4$	B_4	C_4	$^{2,4}A_5$	$^{2,5}A_5$	$^{0,2}A_5$	B_5	C_5	$^{2,4}A_6$	$^{2,5}A_6$	$^{0,2}A_6$	B_6	C_6	$^{2,4}A_7$
dp2	377	161	179	221	263																							
dp3(a)	539	161	179	–	263	–	341	383	425	–																		
dp3(b)	539	161	179	–	–	323	341	383	425	443																		
dp4	665	161	179	–	–	–	341	383	425	443	485	503	545	587	605													
dp5	827	161	179	–	263	–	341	–	425	443	–	503	545	587	605	647	665	707	749	767	809	827	869	911				
dp6(a)	989	161	179	–	263	–	341	383	425	–	–	503	–	587	605	647	665	707	749	767	809	827	869	911				
dp6(b)	989	161	179	–	–	–	341	383	425	443	485	503	545	587	605	–	665	–	–	–	809	827	869	911	929	971	989	1031
dp7	1151	161	179	–	–	–	341	–	425	443	–	503	545	587	605	–	665	–	–	–	809	827	869	911				

[a] The precursor ions of these oligosaccharides are $[M+2H_2O-H]^-$ or $[M-H]^-$.

Table 3
Calculation of linkage types.

	Peak area	$N_{n\ \beta\text{-}(1\ \rightarrow\ 3)}$ [a]	$N_{n\ \beta\text{-}(1\ \rightarrow\ 4)}$ [b]
dp1	237.9	0	1
dp2	307.6	0	2
dp3(a)	57.1	0	3
dp3(b)	670.4	1	2
dp4	664.7	1	3
Ratio [c]		1	3

[a] Number of β-(1 → 3) glucose residues in corresponding oligosaccharide.
[b] Number of β-(1 → 4) glucose residues in corresponding oligosaccharide.
[c] The ratio of β-(1 → 3) to β-(1 → 4) was calculated using the following equation: $\frac{\beta-(1\rightarrow3)}{\beta-(1\rightarrow4)}=\frac{\sum[N_{n\beta}-(1\rightarrow3)\times S_n]}{\sum[N_{n\beta}-(1\rightarrow4)\times S_n]}$.

MS/MS spectra. While, the bond 3 is stabilized but bond 2 is not in the 1 → 4 linked sugar ring. Thus, the bond 2 related cross-ring cleavage ions could be used as diagnostic ions to assign the 1 → 4 linked sugar residue in MS/MS spectra. (Yi, Ouyang et al., 2015; Yi, Sun et al., 2015) Thus, the positions of 1 → 3 and/or 1 → 4 linkages in the oligosaccharides dp2-7 were unambiguously confirmed with MS/MS, and these oligosaccharides in the digested products could be sequenced. In the PAD chromatogram of 6 h aliquot we observed that the peaks were easily grouped, every four peaks starting from that corresponding to dp3(b), as the profile of every four peaks matches (Fig. 2A). This suggests the structural or sequencing pattern, corresponding oligosaccharides in each group, are identical. The first two bigger peaks in every group correspond to 1 → 3/1 → 4 linked heterogeneous oligosaccharides, such as dp3(b)/dp4, G1→3G1→4G/G1→3G1→4G1→4G, and dp6(b)/dp7, G1→3G1→$[4G1]_2$ → 3G1→4G/G1→3G1→$[4G1]_2$ → 3G1→4G1-4G. The other two small peaks correspond to 1 → 4 linked homogeneous oligosaccharides, such as dp5/dp6(a). In the PAD chromatogram of 12 h aliquot, the peaks corresponding to bigger oligosaccharides decreased. In each group, the two peaks corresponding to homogenous oligosaccharides decreased. After 24 h, most large oligosaccharides and the homogenous oligosaccharides larger than dp2 were completely digested, and only glucose, dp2, dp3(b) and dp4 were left. The digestion pattern of this enzyme has been previously reported at 1 → 4 linkages (Ghotra et al., 2008). We could deduce that the most 1 → 4 linked homogeneous domains were degraded to monosaccharide and disaccharides, and most 1 → 3/1 → 4 linked heterogeneous domains were converted to the structures of dp3(b) and dp4 by digestion. Thus, G1→3G1→4G/G1→3G1→4G1→4G are the major repeating blocks of β-glucan, and several homogeneous 1 → 4 linked domains with different lengths occur throughout the whole β-glucan chain.

Moreover, the molar composition of oligosaccharides can be calculated from the ratio of the peak integrations obtained with PAD (Yi, Ouyang et al., 2015). Accordingly, the ratio of 1 → 3 and 1 → 4 linkages in the β-glucan could be roughly calculated as 1:3, (Table 3) which is consistent with the results of ^{13}C NMR.

In this work, the sequences of β-glucan from highland barley were analyzed online with HPACE-PAD-MS/MS. The ratio of 1 → 3 and 1 → 4 linkages was approximately 1:3. It was reported that the ratio of 1 → 3 and 1 → 4 linkages of soluble β-glucan from barley ranged from 2.1 to 2.6 (Aman, 1987; Lee et al., 2015), which is lower than that observed in the β-glucan of highland barley in this work. It implies that this β-glucan has more homogeneous β-(1 → 4) linked segments. The sequences of the β-glucan could be described as that every 1 → 3 linked glucose residue occurs with other two-three 1 → 4 linked glucose residues among the β-glucan chain, but sometimes larger intervals of homogenous 1 → 4 linked glucose domains were observed between 1 → 3 linked glucose residues. The structural and sequencing information of β-glucan from

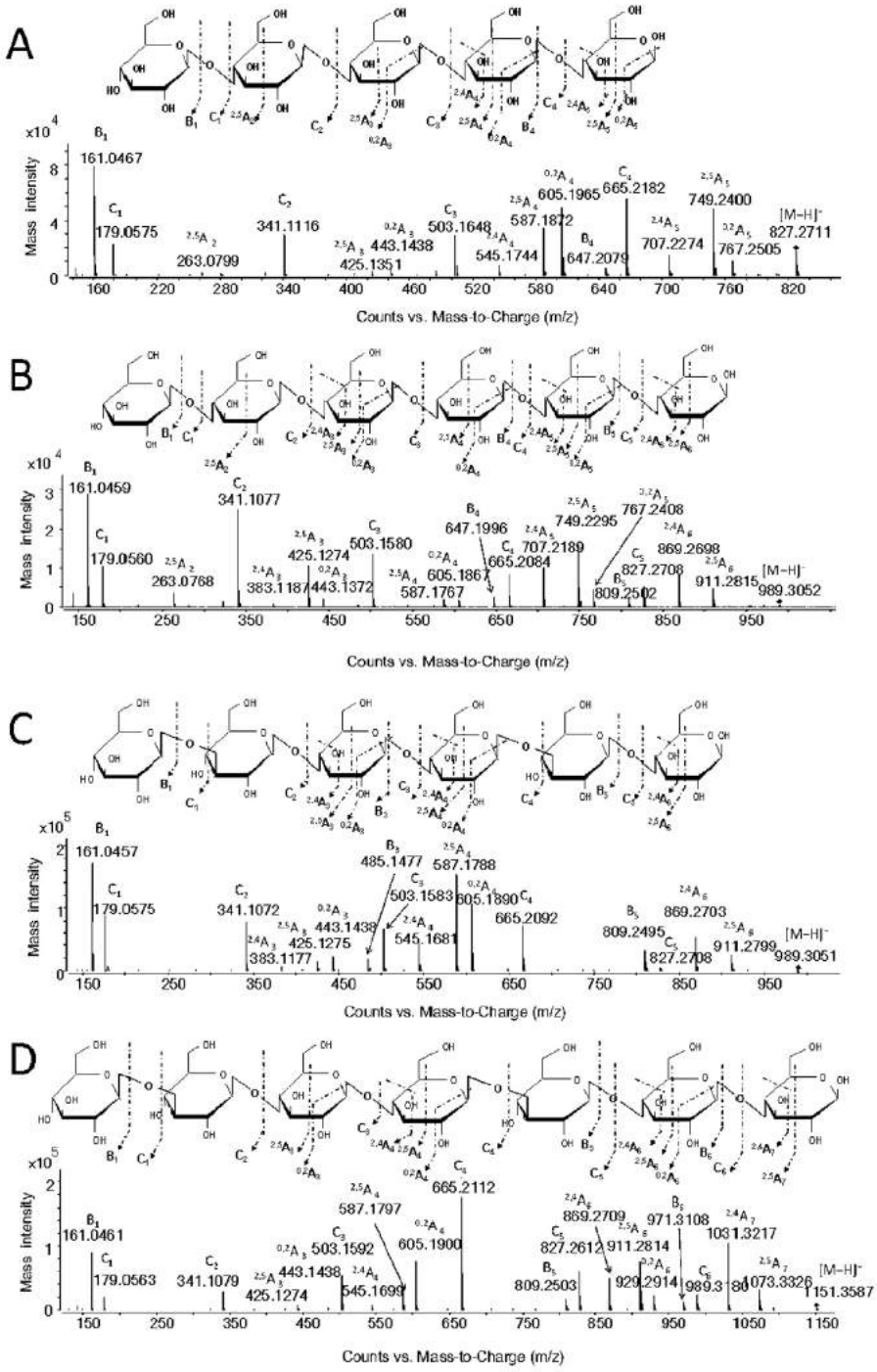

Fig. 4. MS/MS spectra of dp5, dp6 (a), dp6 (b) and dp7.

highland barley elucidated with HPAEC-PAD-MS/MS in this work are much more detailed than those previously reported, such as only linkage ratio analysis with GOPOD determining reagent (Aman, 1987; Lee et al., 2015) or a couple of barley β-glucan derived oligosaccharide (dp3 and dp4) preparation and structural elucidation with HPLC and NMR(Ghotra et al., 2008). This method could be an efficient way to elucidate the detailed structure and sequence of β-glucans from different barleys to estimate the potential relationships between species of barley, detailed structures of β-glucan and corresponding applications.

Acknowledgements

The authors are grateful to the National Natural Science Foundation of China (81473179 and 81673388), and the funding for Jiangsu Key Laboratory of Translational Research and Therapy for Neuro-Psycho-Diseases (BM2013003).

List abbreviation

HPAEC High-performance Anion Exchange Chromatography

PAD	Pulsed Amperemetric Detection
ESI	Electrospray Ion
Q/TOF-MS	Quadrupole time − of − flight Mass Spectrometry
LDL	Low density lipoprotein
LDLR	Low density lipoprotein receptor
NMR	Nuclear Magnetic Resonance
TFA	Trifluoroacetic Acid
CID	The Collision-Induced Dissociation
TIC	Total Ion Chromatograms
EIC	The Extracted Ion Chromatogram
dp	The degree of polymerization
G	Glucose
GOPOD	Glucose Oxidase/Peroxidase

Appendix A. Supplementary data

Supplementary data related to this article can be found at http://dx.doi.org/10.1016/j.foodhyd.2017.07.006.

References

Aman, P. G. H. (1987). Analysis of total and insoluble mixed-linked (1-3), (1-4)- D-glucans in barley and oats. *Journal of Agricultural and Food Chemistry, 35*, 704–709.

Åman, P. (2006). Cholesterol-lowering effects of barley dietary fiber in humans: Scientific support for a generic health claim. *Scandinavian Journal of Nutrition, 50*, 173–176.

Anderson, J. W., Gilinsky, N. H., Deakins, D. A., Smith, S. F., O'Neal, D. S., Dillon, D. W., et al. (1991). Lipid responses of hypercholesterolemic men to oat-bran and wheat-bran intake. *The American Journal of Clinical Nutrition, 54*, 678–683.

Bae, I. Y., Kim, S. M., Lee, S., & Lee, H. G. (2010). Effect of enzymatic hydrolysis on cholesterol-lowering activity of oat beta-glucan. *New Biotechnology, 27*, 85–88.

Bae, I. Y., Lee, S., Kim, S. M., & Lee, H. G. (2009). Effect of partially hydrolyzed oat β-glucan on the weight gain and lipid profile of mice. *Food Hydrocolloids, 23*, 2016–2021.

Domon, B. (1988). A systematic nomenclature for carbohydrate fragmentations in FAB-MS/MS spectra of glycoconjugates. *Glycoconjugate, 5*, 397–409.

Dong, J., Cai, F., Shen, R., & Liu, Y. (2011). Hypoglycaemic effects and inhibitory effect on intestinal disaccharidases of oat beta-glucan in streptozotocin-induced diabetic mice. *Food Chemistry, 129*, 1066–1071.

Drozdowski, L. A., Reimer, R. A., Temelli, F., Bell, R. C., Vasanthan, T., & Thomson, A. B. (2010). Beta-glucan extracts inhibit the in vitro intestinal uptake of long-chain fatty acids and cholesterol and down-regulate genes involved in lipogenesis and lipid transport in rats. *Journal of Nutritional Biochemistry, 21*, 695–701.

Gangopadhyay, N., Hossain, M. B., Rai, D. K., & Brunton, N. P. (2015). A review of extraction and analysis of bioactives in oat and barley and scope for use of novel food processing Technologies. *Molecules, 20*, 10884–10909.

Ghotra, B. S., Vasanthan, T., & Temelli, F. (2008). Structural characterization of barley β-glucan extracted using a novel fractionation technique. *Food Research International, 41*, 957–963.

Ibrugger, S., Kristensen, M., Poulsen, M. W., Mikkelsen, M. S., Ejsing, J., Jespersen, B. M., et al. (2013). Extracted oat and barley beta-glucans do not affect cholesterol metabolism in young healthy adults. *Journal of Nutrition, 143*, 1579–1585.

Idstrom, A., Schantz, S., Sundberg, J., Chmelka, B. F., Gatenholm, P., & Nordstierna, L. (2016). (13)C NMR assignments of regenerated cellulose from solid-state 2D NMR spectroscopy. *Carbohydr Polym, 151*, 480–487.

Johansson, L., Virkkia, L., Maunu, S., Lehto, M., Ekholm, P., & Varo, P. (2000). Structural characterization of water soluble b-glucan of oat bran. *Carbohydrate Polymers, 42*, 143–148.

Lam, K.-L., & Chi-Keung Cheung, P. (2013). Non-digestible long chain beta-glucans as novel prebiotics. *Bioactive Carbohydrates and Dietary Fibre, 2*, 45–64.

Lee, S. H., Jang, G. Y., Hwang, I. G., Kim, H. Y., Woo, K. S., Kim, K. J., et al. (2015). Physicochemical properties of β-glucan from acid hydrolyzed barley. *Preventive Nutrition and Food Science, 20*, 110–118.

Lehtovaara, B. C., & Gu, F. X. (2011). Pharmacological, structural, and drug delivery properties and applications of 1,3-beta-glucans. *Journal of Agricultural and Food Chemistry, 59*, 6813–6828.

Liu, M., Zhang, Y., Zhang, H., Hu, B., Wang, L., Qian, H., et al. (2016). The anti-diabetic activity of oat beta-d-glucan in streptozotocin-nicotinamide induced diabetic mice. *International Journal of Biological Macromolecules, 91*, 1170–1176.

Lopez-Sanchez, P., Wang, D., Zhang, Z., Flanagan, B., & Gidley, M. J. (2016). Microstructure and mechanical properties of arabinoxylan and (1,3;1,4)-β-glucan gels produced by cryo-gelation. *Carbohydrate Polymers, 151*, 862–870.

Mikkelsen, M. S., Jespersen, B. M., Larsen, F. H., Blennow, A., & Engelsen, S. B. (2013). Molecular structure of large-scale extracted beta-glucan from barley and oat: Identification of a significantly changed block structure in a high beta-glucan barley mutant. *Food Chemistry, 136*, 130–138.

Peng, F., Peng, P., Xu, F., & Sun, R. C. (2012). Fractional purification and bioconversion of hemicelluloses. *Biotechnology Advances, 30*, 879–903.

Razzaq, H. A. A., Pezzuto, M., Santagata, G., Silvestre, C., Cimmino, S., Larsen, N., et al. (2016). Barley β-glucan-protein based bioplastic film with enhanced physicochemical properties for packaging. *Food Hydrocolloids, 58*, 276–283.

Schmidt, E. P., Overdier, K. H., Sun, X., Lin, L., Liu, X., Yang, Y., et al. (2016). Urinary glycosaminoglycans predict outcomes in septic shock and acute respiratory distress syndrome. *American Journal of Respiratory and Critical Care Medicine, 194*, 439–449.

Schulze, C., Wetzel, M., Reinhardt, J., Schmidt, M., Felten, L., & Mundt, S. (2016). Screening of microalgae for primary metabolites including β-glucans and the influence of nitrate starvation and irradiance on β-glucan production. *Journal of Applied Phycology, 28*, 2719–2725.

Shao, Y., Wang, Z., Tian, X., Guo, Y., & Zhang, H. (2016). Yeast beta-d-glucans induced antimicrobial peptide expressions against Salmonella infection in broiler chickens. *International Journal of Biological Macromolecules, 85*, 573–584.

Thondre, P. S., & Henry, C. J. (2009). High-molecular-weight barley beta-glucan in chapatis (unleavened Indian flatbread) lowers glycemic index. *Nutrition Research, 29*, 480–486.

Tiwari, U., & Cummins, E. (2011). Meta-analysis of the effect of beta-glucan intake on blood cholesterol and glucose levels. *Nutrition, 27*, 1008–1016.

Tong, L. T., Zhong, K., Liu, L., Zhou, X., Qiu, J., & Zhou, S. (2015). Effects of dietary hull-less barley beta-glucan on the cholesterol metabolism of hypercholesterolemic hamsters. *Food Chemistry, 169*, 344–349.

Tosh, S. (2004). Evaluation of structure in the formation of gels by structurally diverse (1-3)(1-4)-d–glucans from four cereal and one lichen species. *Carbohydrate Polymers, 57*, 249–259.

Uskoković, A., Mihailović, M., Dinić, S., Arambašić Jovanović, J., Grdović, N., Marković, J., et al. (2013). Administration of a β-glucan-enriched extract activates beneficial hepatic antioxidant and anti-inflammatory mechanisms in streptozotocin-induced diabetic rats. *Journal of Functional Foods, 5*, 1966–1974.

Yang, L., Christensen, D. A., McKinnon, J. J., Beattie, A. D., & Yu, P. (2013). Effect of altered carbohydrate traits in hulless barley (Hordeum vulgare L.) on nutrient profiles and availability and nitrogen to energy synchronization. *Journal of Cereal Science, 58*, 182–190.

Yi, L., Ouyang, Y., Sun, X., Xu, N., Linhardt, R. J., & Zhang, Z. (2015). Qualitative and quantitative analysis of branches in dextran using high-performance anion exchange chromatography coupled to quadrupole time-of-flight mass spectrometry. *Journal of Chromatography A, 1423*, 79–85.

Yi, L., Sun, X., Du, K., Ouyang, Y., Wu, C., Xu, N., et al. (2015). UP-HILIC-MS/MS to determine the action pattern of penicillium sp. Dextranase. *Journal of the American Society for Mass Spectrometry, 26*, 1174–1185.

Yoshida, T., Honda, Y., Tsujimoto, T., Uyama, H., & Azuma, J. (2014). Selective isolation of beta-glucan from corn pericarp hemicelluloses by affinity chromatography on cellulose column. *Carbohydrate Polymers, 111*, 538–542.

Zhang, Z., Khan, N. M., Nunez, K. M., Chess, E. K., & Szabo, C. M. (2012). Complete monosaccharide analysis by high-performance anion-exchange chromatography with pulsed amperometric detection. *Analytical Chemistry, 84*, 4104–4110.

Zhao, J., & Cheung, P. C. (2013). Comparative proteome analysis of Bifidobacterium longum subsp. infantis grown on beta-glucans from different sources and a model for their utilization. *Journal of Agricultural and Food Chemistry, 61*, 4360–4370.

Zhu, F., Du, B., & Xu, B. (2015). Superfine grinding improves functional properties and antioxidant capacities of bran dietary fibre from Qingke (hull-less barley) grown in Qinghai-Tibet Plateau, China. *Journal of Cereal Science, 65*, 43–47.

Zhu, X., Sun, X., Wang, M., Zhang, C., Cao, Y., Mo, G., et al. (2015). Quantitative assessment of the effects of beta-glucan consumption on serum lipid profile and glucose level in hypercholesterolemic subjects. *Nutrition, Metabolism & Cardiovascular Diseases, 25*, 714–723.